EurJOC
European Journal of Organic Chemistry

Full Papers
doi.org/10.1002/ejoc.202100014

Chemistry Europe
European Chemical Societies Publishing

Special Collection

The Role of Chain Length in Cucurbit[8]uril Complexation of Methyl Alkyl Viologens

Alessandro Pedrini,[a] Anjali Devi Das,[a] Roberta Pinalli,[a] Neal Hickey,[b] Silvano Geremia,[b] and Enrico Dalcanale*[a]

Dedicated to Prof. Franco Cozzi in occasion of his 70th birthday.

Viologens are among the most studied guests for cucurbit[8]uril (**CB[8]**) and their complexation is usually driven by bipyridyl core inclusion inside the cavity to maximize both hydrophobic and cation-dipole interactions. The presence of alkyl substituents on the guest alters this complexation mode, switching to aliphatic chain inclusion in U-folded conformation. Herein, we report a thorough study of the influence of the alkyl chain length on the binding mode of methyl alkyl viologens. The chain length of the studied guests was increased by two methylene groups starting from methyl dodecyl viologen (**MVC12**) to the octadecyl analogue (**MVC18**). Complexation in water, investigated by NMR spectroscopy and ITC, revealed a clear switch from 1:1 to 2:1 host/guest stoichiometry moving from 12 to 16 carbon atoms, as a consequence of the chain folding of the major portion of the longer alkyl chain in one **CB[8]** cavity and the inclusion of the full viologen unit by another host molecule. The **CB[8]$_2$•MVC18** complex crystal structure evidences the unprecedented 2:1 stoichiometry and quantified in 12 the number of carbon atoms necessary to fill the **CB[8]** cavity in U-shaped conformation.

Introduction

Cucurbit[n]urils are an important class of molecular receptors featuring exceptional complexation properties in water.[1–5] Their complexation behavior depends on the diameter of the toroidal cavity, defined by the number of glycoluril units connected. Among the CB[n] family, **CB[8]** stands out as the less predictable in terms of complex stoichiometry, having the ability to form 1:1 binary,[6] 2:1 homoternary, 1:1:1 heteroternary,[7] 2:2 quaternary[8] and 3:2 quinternary[9] complexes, as well as discrete (n:n) host-guest oligomers.[10] The knowledge of the exact binding mode of **CB[8]** complexes impacts on their assembly mode and on their properties, such as fluorescence emission.[11]

Viologens are among the most studied guests for **CB[8]** complexation, thanks to their two positive charges separated by an aromatic hydrophobic region. These cations bind to the carbonyl portals through cation-dipole interactions, while the bipyridine core interacts with the **CB[8]** cavity via hydrophobic interactions. This bimodal interaction mode leads to high binding affinity in water. The progenitor methyl viologen (**MV**), also known as paraquat, binds to **CB[8]** in a 1:1 stoichiometry with a log K of 5.04.[12]

In the solid state, the substitution of the methyl groups with either one or two long aliphatic chains alters the binding mode substantially. For instance, dialkylated viologens form supramolecular polymers by inclusion of two short (C6) alkyl chains from distinct molecules in one **CB[8]** cavity.[13] Analogously, connecting two viologen cores with linear alkyl chains (C6 and C8) leads to the formation of a novel supramolecular polymer with two **CB[8]** hosts involved in guest complexation: one threads the alkyl spacer between the aromatic cores while the other is involved in the propagation of the supramolecular polymer by complexing two terminal butyl chains of distinct guest molecules.[14]

In aqueous solution, **MV** derivatives are typically used as electron-deficient acceptor molecule in the construction of heteroternary complexes with a second electron-rich guest.[7] As unique characteristic of **CB[8]**, the formation of these complexes by host-enhanced charge transfer has been extensively exploited as a "molecular handcuff"[15] for the permanent linking of extended architectures.[16–18] In particular, ditopic viologen-based monomers have been involved in the preparation of both linear and cyclic supramolecular polymers,[19–22] while the decoration of polymeric backbones[23–25] and surfaces[26,27] with appended viologen units revealed to be extremely efficient in the preparation of supramolecular hydrogels and adhesives. Moreover, asymmetrically alkylated viologens can provide, by heteroternary complexation, supramolecular amphiphiles that are capable to convert micelles in vesicles.[28–32] In all these applications the viologen species interact with **CB[8]** mainly with their aromatic core. Methyl decyl viologen, instead, forms a 1:1 host-guest complex with **CB[8]**, where the long alkyl

[a] Dr. A. Pedrini, Dr. A. Devi Das, Prof. R. Pinalli, Prof. E. Dalcanale
Department of Chemistry, Life Science and Environmental Sustainability
University of Parma
Parco Area delle Scienze 17/A, 43124 Parma, Italy
E-mail: enrico.dalcanale@unipr.it
www.dalcanalegroup.unipr.it
[b] Dr. N. Hickey, Prof. S. Geremia
Centre of Excellence in Biocrystallography, Department of Chemical and Pharmaceutical Sciences
University of Trieste
Via L. Giorgieri 1, 34127 Trieste, Italy

Supporting information for this article is available on the WWW under https://doi.org/10.1002/ejoc.202100014

Part of the "Franco Cozzi's 70th Birthday" Special Collection.

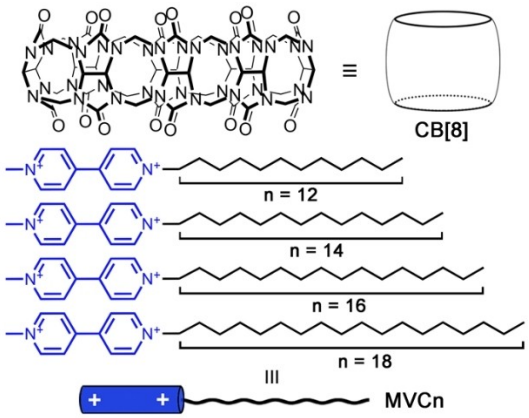

Scheme 1. Structure of cucurbit[8]uril (**CB[8]**) and methyl alkyl viologen dichloride salts (**MVCn**) involved in this study.

chain is in a folded conformation inside the host cavity.[33] The C10 chain adopts a U-shaped conformation inside the **CB[8]** cavity while the viologen group resides outside the **CB[8]** cavity, as confirmed by X-ray crystal structure analysis.

A deep understanding of complexation modes and equilibria involved in alkyl viologens complexation by **CB[8]** is of high interest for the control of the above mentioned self-assembled architectures. In particular, the dual capability of these guest to interact with the cavity with either their aromatic core or the folded aliphatic chain needs to be further investigated. Here we report the analysis of the influence of the alkyl chain length on the binding mode of methyl alkyl viologens with **CB[8]** (Scheme 1). In water, a clear switch from 1:1 to 2:1 stoichiometry is observed upon moving from 12 to 16 carbon atoms. This switch is attributed to the longer alkyl chain, which allows both the chain folding in one **CB[8]** cavity and the viologen binding by another.

Results and Discussion

Synthesis of the host and the guests. **CB[8]** was prepared by acid-catalyzed condensation of glycoluril with formaldehyde and purified by repeated precipitations following a well-established reported procedure.[34] To determine the influence of alkyl chain length in the complexation with **CB[8]**, four methyl viologens derivatives (**MVCn**, Scheme 1) were synthesized following literature procedures.[35] The guests were obtained as iodide-bromide salts reacting 1-methyl-4-bipyridinium iodide with the corresponding alkyl bromide. The chain length was increased each time by two methylene groups starting from dodecyl methyl viologen (**MVC12**) to the octadecyl analogue (**MVC18**). These guests were used as synthesized for crystals growth experiments. To increase their limited solubility in water, the counterions were exchanged with chlorides before performing solution experiments.

Solution studies. The influence of the alkyl chain length extension in **MVCn** complexation by **CB[8]** in solution was investigated *via* nuclear magnetic resonance (NMR) spectroscopy and isothermal titration calorimetry (ITC).

NMR titration experiments were performed recording ^{1}H NMR spectra of a 0.3 mM solution of **MVCn** salts in D_2O in the presence of incremental equivalents of **CB[8]** (Figure S1-3 and Figure 1).

The complexation of **MVC12** follows a trend similar to the one reported for the decyl counterpart up to 1 eq of **CB[8]**,[15] leading to the formation of a complex with a 1:1 stoichiometry. The addition of the second equivalent causes a further upfield of the viologen signals, indicating a deeper inclusion of this part in the cavity balanced by a small downfield shift of the signals related to aliphatic protons (Figure S1), with no evidence of complexation stoichiometry perturbation. NMR titration of **MVC14** presents a similar trend (Figure S2). When present in deficit (0.5 eq) **CB[8]** is prone to interact with both terminus of the molecule, leaving the signals of the central methylene groups (1-3) almost unaltered. The system then moves to a 1:1 complex that includes only the U-folded alkylated end of the viologen upon increasing the concentration of the **CB[8]** up to 2 eq. The titration outcome is completely different with longer **MCVn** counterparts: the addition of 0.5 eq of the host causes the broadening of **MVC18** signals (Figure 1b), as already observed for similar guests in fast exchange between bound and unbound forms.[8] When **CB[8]** is present in equimolar amount, instead, the guest signals present a more defined pattern (Figure 1c): the peaks of the aliphatic portion are shifted upfield and tends to differentiate one from the other, while signals for the viologen unit are split over more than 1 ppm region. These complexation-induced shifts are consistent with a 1:1 complex bearing a U-shaped alkyl tail, as already observed for methyl alkyl viologen salts with shorter chains. In the case of **MVC18**, however, the terminal CH_3 group does not reach negative ppm indicating that the methyl group is less buried inside the **CB[8]** cavity. The addition of a second equivalent of the host further modifies the NMR spectrum of the solution (Figure 1d). The triplet of methylene 1, which was upfield

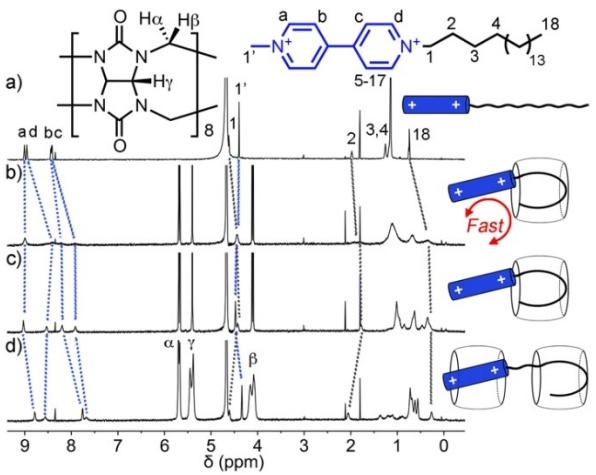

Figure 1. ^{1}H NMR (600 MHz, D_2O, 278 K) spectra of 0.3 mM solution of free guest **MVC18** (a) and in the presence of 0.5 (b), 1.0 (c) and 2.0 (d) equivalents of **CB[8]**. Colored dotted lines are added to guide the reader.

shifted in the previous spectra as a consequence of its inclusion in the **CB[8]** cavity *via* interactions between the positively charged nitrogen atom of the guest and the carbonyl groups present at the host rims, returns to its initial position indicating the decomplexation of this part of the guest. The increased perturbation of viologen signals suggests a deeper inclusion of this part in the host cavity. Interestingly, the signals of **CB[8]** external protons are also split, indicating two different complexation modes for the host. **MVC16** follows a similar behavior, with NMR spectra compatible with a 2:1 complex (Figure S3).

ITC experiments were performed to further assess complex stoichiometries, together with thermodynamic parameters ΔH, K_a, ΔG, and ΔS associated with the complexation processes. Due to the limited **CB[8]** solubility in water, these titration were performed in a reverse fashion compared to NMR titration: to a 0.1 mM water solution of **CB[8]** placed in the cell, 38 aliquots of a 1.0 mM water solution of each **MVCn** were added to reach molar ratios close to 2 (Figure S4-7). Integration of the peaks obtained from the heat released as a consequence of the complexation event afforded the binding curve. The binding isotherms of the integrated calorimetric titration data of each guest are compared in Figure 2. For all the four titrations, two

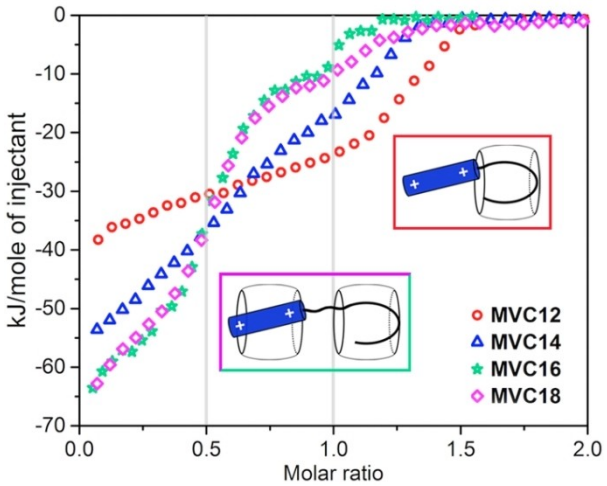

Figure 2. Binding isotherms resulting from calorimetric titration data for **CB[8]** and methyl alkyl viologen dichloride salts (**MVCn**). The integrated heat change per injection, normalized by the amount of guest injected, is reported as a function of the molar ratio of guest/host in the sample cell for all the four studied systems.

inflection points are detectable, one at molar ratio close to 0.5 and the other at 1. These steps-like curves are ascribable to the presence of two different interaction mechanisms, through the viologen unit and through the alkyl chain, on **MVCn** molecules, which therefore behave as bifunctional guests.

The marked preference for the formation of a 1:1 complex for **MVC12** is clearly evidenced by the negligible contribution of the first event in the titration. The best fitting for this curve was obtained applying a "one set of sites" model, as reported in Table 1.

In the case of **MVC18** and **MVC16**, which present similar curve shapes, 2:1 complexes are formed in solution with the inclusion of both the viologen and the folded chain. The first binding event occurs in the presence of 2 eq. of **CB[8]** for each guest (situation analogous to the last spectrum in NMR experiments). Further addition of the guest causes the reorganization of the system towards the formation of a 1:1 complex comprising the U-shaped alkyl chain. This process is completed at molar ratios higher than 1 (second inflection point). The **MVC14** curve, instead, presents an intermediate situation. Following these considerations, we decided to apply the "two sets of sites" model to the fitting of the binding curves. The variation of these contributions for the two events along the series nicely matches the effect of the longer alkyl chain, which promotes the 2:1 complex stoichiometry.

Further support to the formation of 2:1 complexes in water was obtained by Diffusion Ordered Spectroscopy (DOSY) NMR. DOSY-NMR is a well-established technique for the estimation of hydrodynamic radius (r) of supramolecular assemblies in solution. From measured diffusion coefficients (D), r can be calculated applying the Stokes-Einstein equation ($D = k_b T/6\pi\eta r$) with the assumption that the species in solution is spherical.

DOSY-NMR experiments were performed on 0.3 mM solution of **MVCn** salts in D_2O in the presence of 2 equivalents of **CB[8]**. The obtained r value, which accounts for the whole solvation sphere of the species, are reported in Table 2. Diffusion coefficients measured with **MCV16** and **MCV18** guests are in line with those observed for 2:2 complexes[10] and the calculated hydrodynamic radii nicely match with the involvement of two macrocycles in the formation of the supramolecular entities. On the other hand, the r value obtained upon complexation of **MVC12** is in agreement with the formation of a smaller 1:1 complex, even in the presence of an excess of **CB[8]**. For **MVC14**, instead, an intermediate

Table 1. Thermodynamic data obtained from ITC experiments for the complexation of **MVCn** as guest with **CB[8]** as host, measured in water solution at 298 K.[a]

Guest	n	K_a [M^{-1}]	ΔH [kJ/mol]	ΔG [kJ/mol]	$T\Delta S$ [kJ/mol]
MVC12	1.12 (±0.02)	$7.3\ (\pm0.3)\times10^6$	−39.2 (±0.8)	−39.1 (±0.5)	−0.11 (±0.03)
	/	/	/	/	/
MVC14	1.07 (±0.02)	$4.8\ (\pm0.2)\times10^4$	−17.3 (±0.6)	−26.7 (±0.1)	9.4 (±0.3)
	0.91 (±0.01)	$9.1\ (\pm0.8)\times10^6$	−37.6 (±0.5)	−39.6 (±0.3)	2.1 (±0.2)
MVC16	1.09 (±0.01)	$9.7\ (\pm0.2)\times10^4$	−25.2 (±0.7)	−28.3 (±0.5)	3.2 (±0.9)
	0.97 (±0.02)	$8.6\ (\pm0.9)\times10^7$	−33.3 (±0.3)	−45.4 (±0.3)	11.8 (±0.1)
MVC18	1.08 (±0.01)	$1.4\ (\pm0.4)\times10^5$	−22.5 (±1)	−29.4 (±0.8)	6.9 (±0.2)
	0.97 (±0.01)	$2.4\ (\pm0.5)\times10^7$	−32.3 (±0.4)	−42.2 (±0.7)	8.9 (±0.3)

[a] Reported error values correspond to the standard deviation of at least three different measurements.

Table 2. Diffusion coefficients (*D*) and hydrodynamic radius (*r*) obtained for DOSY-NMR experiments.

	D [m²/s]	r [Å]
CB[8]•MVC12	$2.7\ (\pm 0.1)\times 10^{-10}$	8
$CB[8]_x$•MVC14	$1.9\ (\pm 0.1)\times 10^{-10}$	11
$CB[8]_2$•MVC16	$1.6\ (\pm 0.1)\times 10^{-10}$	13
$CB[8]_2$•MVC18	$1.5\ (\pm 0.1)\times 10^{-10}$	14

diffusion coefficient value was obtained, suggesting the presence of an equilibrium between the two complexation modes.

Crystal structures. The observation of a well-defined 2:1 stoichiometry for the complexation of **MVC18** in solution prompted us to investigate the nature of this complex in the solid state.

Small pale pink single crystals of **$CB[8]_2$•MVC18** were analyzed at the XRD1 beamline of the Elettra synchrotron using cryo-cooling techniques. The asymmetric unit of the monoclinic crystals ($P2_1$ space group) contains one 2:1 **$CB[8]_2$•MVC18** complex with its four bromine counter-ions and 44.5 water molecules. The aromatic head of **MVC18** is complexed by one **CB[8]** molecule, while the last 12 carbon atoms of the aliphatic tail are hosted by the second macro-ring, adopting a hook-like conformation (Figure 3a). The terminal pyridinium group of **MVC18** interacts with the carbonyl groups of **CB[8]** through charge–dipole interactions, with the shortest N···O distance of 3.32 Å. The viologen group is hosted by an ideal $D8_h$ symmetric **CB[8]** molecule in an asymmetric manner, with the center of the host at 1.68 Å from the pyridine mean plane. This pyridine plane is oriented orthogonally with respect to the mean plane of the portal oxygen atoms (89.5°). The N atom is located inside the macro-ring at a distance of 0.71 Å from this **CB[8]** portal plane. The two pyridinium moieties of the viologen group are mutually rotated by 31.4°. The internal pyridinium group also

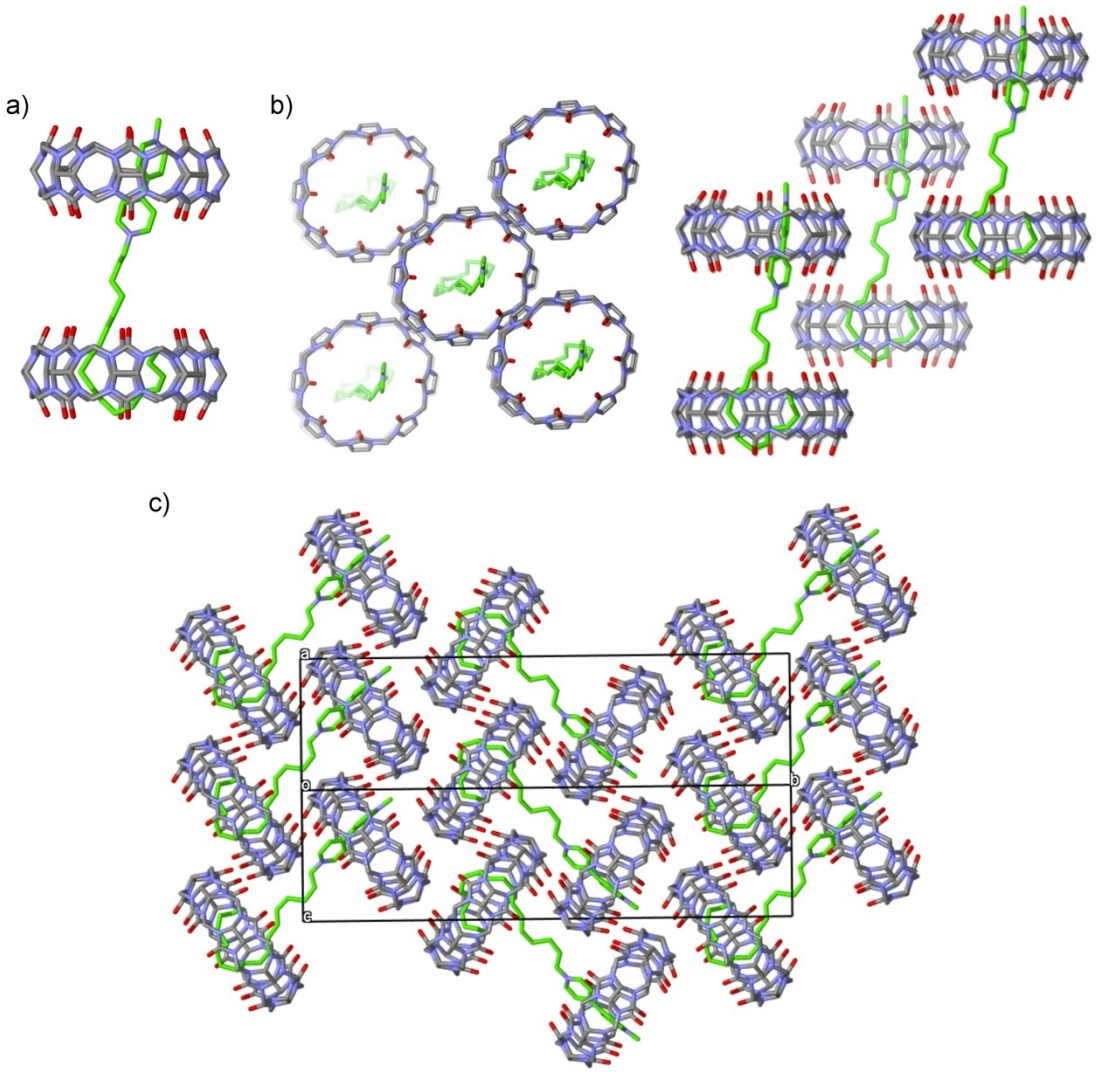

Figure 3. Stick representations of the crystal structure of **$CB[8]_2$•MVC18**. a) side view of the 2:1 **$CB[8]_2$•MVC18** complex presents in the asymmetric unit. b) orthogonal views of the square arrangement of the four 2:1 complexes surrounding the **MVC18** alkyl chain of the central 2:1 complex. Two pairs of the complexes are overlapped in the side view. c) Crystal packing, as viewed along the ac direction. The atomic species are represented in CPK colors with the exception of the **MVC18** carbon atoms, which are colored in green. Hydrogen atoms, water molecules and counter-anions are omitted for clarity.

interacts with the carbonyl groups of **CB[8]**, with the shortest N···O distance of 3.38 Å. However, its positively charged N atom is located outside the macro-ring at a distance of 1.29 Å from the second **CB[8]** portal plane (Figure 3a). For comparison, in the previous reported 1:1 **CB[8]•MVC10** the complexation of the viologen group is completely different.[33] In that case, the viologen moiety is partially outside the macro ring (the out of plane distance of the terminal positive N atom from the O-portal is 2.06 Å) and is leaning to its portal with an angle of about 37°.

The aliphatic chain of **MVC18** assumes a chiral helical conformation with the above-mentioned hook-shaped terminal (Figure 3b). The complete conformation of the alkyl chain is A^+–T^-–G^-–T^+–G^+–T^+–T^+–T^-–G^-–G^-–T^+–G^-–G^-–T^+–A^-–C^+–A^- (C = cis, G = gauche, A = anticlinal, T = trans, with the sign of the torsion angle in superscript) with the position of the last nine carbon atoms affected by high anisotropic thermal motions. An analogous U-shape conformation of the terminal part of the alkyl chain was observed in several complexes of **CB[8]** with alkyl-derivatives featuring long linear chains.[36,37]

The absolute chirality of the non-centrosymmetric $P2_1$ crystal was determined by the Flack parameter of 0.104(3) using 15869 quotients [(I+)-(I-)]/[(I+)+(I-)]. A chiral conformation assumed by a guest within this $D8_h$ symmetric host is not unprecedented.[36,38,39] The crystals of three different host–guest complexes between **CB[8]** and alkyltrimethylammonium ions (C_8TA^+, $C_{10}TA^+$ and $C_{12}TA^+$) all belong to the non-centrosymmetric $P2_1$ space group.[36]

In the present structure, the distance between the two facing **CB[8]** portals of the 2:1 complex is 8.15 Å. The open space, 5.11 Å wide (considering the vdW radii of the O atoms), which contains the central alkyl chain of **MVC18**, is only partially filled by a square arrangement of four surrounding **CB[8]** hosts (Figure 3b). In fact, the height of the **CB[8]** molecules is significantly larger than the open space between the facing **CB[8]** portals (mean value of 9.18 Å considering the vdW radii of the O atoms). This arrangement produces a 2D assembly of the 2:1 complexes lying on the ac plane of the crystal (Figure 3c). Alternate slices of this 2D assembly, symmetrically related by 2_1 screw axes, pack orthogonally along the b direction of the crystal (Figure 3c). Therefore, this crystal packing stabilizes the conformation of the central **MVC18** alkyl chain and the overall architecture of the 2:1 complex with two aligned host molecules.

Conclusion

The present work clarifies the role of the alkyl chain length on the complexation mode of methyl alkyl viologens by **CB[8]**. The primary interaction mode is the U-shaped folding of the alkyl chain within one **CB[8]**, which requires 12 methylene units to fill the cavity, as shown by the crystal structure of **CB[8]$_2$•MVC18**. The K_a of this complexation is in the range 10^6–10^7 M^{-1}, as determined by ITC measurements. The inclusion of the methyl viologen unit by another **CB[8]** requires the presence of at least four additional methylene units to be fully effective. Shorter linkers make this second interaction sterically unfavorable. Accordingly, ITC measurements show a progressive increase of this second complexation event from 4.8×10^4 to 1.4×10^5 M^{-1} moving from **MVC14** to **MVC18**. The 2:1 complexation mode is operative both in solution and in the solid state for **MVC18**, as demonstrated by the combination of NMR and ITC titrations, DOSY measurements and the crystal structure of **CB[8]$_2$•MVC18**.

Experimental Section

Synthesis. All starting materials were purchased from commercial sources and used as received. **CB[8]** was synthetized and purified following a published procedure.[34] Its purity was determined to be 80% via ITC, titrating a solution of **CB[8]** in sodium acetate buffer (pH = 4.65) with 1-adamantylamine.[8] **MVCn** guests were obtained as bromide/iodide salts reacting 1-methyl-4-bipyridinium iodide with the corresponding alkyl bromide, following a previously reported procedure.[35] For solution studies in water, the counter-ions were exchanged with chlorides by passing methanol solutions of the guests through Amberlite® IRA-400 resin (chloride form).

Single-crystal X-ray diffraction spectroscopy (SC-XRD). Single crystals suitable for an X-ray investigation were obtained by slowly cooling a boiling water solution of **CB[8]** and **MVC18.** Data collection was carried out at the Macromolecular crystallography XRD1 beamline of the Elettra synchrotron (Trieste, Italy), employing the rotating-crystal method with a Dectris Pilatus 2 M area detector. Single crystals were dipped in paratone cryoprotectant, mounted on a nylon loop and flash-frozen under a nitrogen stream at a 100 K. Diffraction data were indexed and integrated using the XDS package,[40] while scaling was carried out with XSCALE.[41] Structures was solved using the SHELXT program.[42] The asymmetric unit of the monoclinic ($P2_1$ space group) crystals of **CB[8]$_2$•MVC18** is composed of two **CB[8]** molecules, one **MVC18** molecule, two bromine counter-ions statistically distributed over 6 sites and 44.5 partially disordered water molecules. The structure was refined with SHELXL-18/3,[43] operating through the WinGX GUI,[44] by full-matrix least-squares (FMLS) methods on F^2. Non-hydrogen atoms were refined anisotropically, with the exception of some water molecules with occupancy factors below 0.5. Excluding the water molecules, hydrogen atoms were added at the calculated positions and refined using the riding model. Crystallographic data and refinement details are reported in Table S1.

Nuclear magnetic resonance spectroscopy (NMR). ^{1}H NMR spectra were obtained using a 400 MHz Bruker AVANCE or a 600 MHz JEOL spectrometer. All chemical shifts (δ) were reported in ppm relative to the proton resonances resulting from the incomplete deuteration of the NMR solvents. Diffusion-ordered NMR spectroscopy (DOSY) spectra were acquired at 17.6 °C on a 600 MHz JEOL spectrometer. The spectra were acquired with a bbp_led_dosy_pfg sequence with gradient spoiling, using 800 scans. The gradient strength was logarithmic incremented of 14 steps from 30 to 600 mT/m. Diffusion time was set to 0.12 s, delta was 2 ms and the relaxation delay was 10 s. Diffusion coefficient values were obtained by fitting peak intensity decays in Delta 5.3.0 software using the curve analysis option.

Isothermal titration calorimetry (ITC). Titrations were performed in water at 25 °C on a MicroCal PEAQ-ITC System. The ITC titrations were performed by adding incremental amounts of **MVCn** to a solution of **CB[8]** placed in the cell of the calorimeter. Stoichiometry and thermodynamic parameters were calculated as the average of three experiments. The heat released upon binding was tracked

against time (top trace). To account for unspecific heats of dilution, **MVCn** were also titrated into pure water (blank titrations) affording no significant heat.

Deposition Number 2033336 (for **CB[8]$_2$•MVC18**) contains the supplementary crystallographic data for this paper. These data are provided free of charge by the joint Cambridge Crystallographic Data Centre and Fachinformationszentrum Karlsruhe Access Structures service www.ccdc.cam.ac.uk/structures.

Acknowledgements

This work has benefited from the equipment and framework of the COMP-HUB Initiative, funded by the 'Departments of Excellence' program of the Italian Ministry for Education, University and Research (MIUR, 2018–2022). The authors acknowledge for financial support MIUR through the PRIN project 20179BJNA2. The authors acknowledge the Centro Interfacoltà di Misure "G. Casnati" of the University of Parma for the use of NMR facilities and Dr. Stefano Ghelli for the support in DOSY experiments. AP acknowledges Prof. Pablo Ballester for the fruitful discussion on ITC measurements.

Conflict of Interest

The authors declare no conflict of interest.

Keywords: Complex stoichiometry · Crystal structure · Cucurbit [8]uril · Host-guest complexation · Viologens

[1] J. W. Lee, S. Samal, N. Selvapalam, H. J. Kim, K. Kim, *Acc. Chem. Res.* **2003**, *36*, 621–630.
[2] J. Lagona, P. Mukhopadhyay, S. Chakrabarti, L. Isaacs, *Angew. Chem. Int. Ed.* **2005**, *44*, 4844–4870; *Angew. Chem.* **2005**, *117*, 4922–4949.
[3] E. Masson, X. Ling, R. Joseph, L. Kyeremeh-Mensah, X. Lu, *RSC Adv.* **2012**, *2*, 1213–1247.
[4] S. J. Barrow, S. Kasera, M. J. Rowland, J. Del Barrio, O. A. Scherman, *Chem. Rev.* **2015**, *115*, 12320–12406.
[5] K. I. Assaf, W. M. Nau, *Chem. Soc. Rev.* **2015**, *44*, 394–418.
[6] D. Sigwalt, M. Šekutor, L. Cao, P. Y. Zavalij, J. Hostaš, H. Ajani, P. Hobza, K. Mlinarić-Majerski, R. Glaser, L. Isaacs, *J. Am. Chem. Soc.* **2017**, *139*, 3249–3258.
[7] Y. H. Ko, E. Kim, I. Hwang, K. Kim, *Chem. Commun.* **2007**, 1305–1315.
[8] G. Wu, M. Olesińska, Y. Wu, D. Matak-Vinkovic, O. A. Scherman, *J. Am. Chem. Soc.* **2017**, *139*, 3202–3208.
[9] G. Wu, I. Szabó, E. Rosta, O. A. Scherman, *Chem. Commun.* **2019**, *55*, 13227–13230.
[10] X. Yang, R. Wang, A. Kermagoret, D. Bardelang, *Angew. Chem. Int. Ed.* **2020**, *59*, 21280–21292.
[11] X. Zhang, T. Sun, X.-L. Ni, *Org. Chem. Front.* **2020**, DOI 10.1039/d0qo00649a.
[12] W. S. Jeon, H. J. Kim, C. Lee, K. Kim, *Chem. Commun.* **2002**, 1828–1829.
[13] X. Xiao, R. L. Lin, L. M. Zheng, W. Q. Sun, Z. Tao, S. F. Xue, Q. J. Zhu, J. X. Liu, *RSC Adv.* **2014**, *4*, 53665–53668.
[14] X. Xiao, N. Sun, D. Qi, J. Jiang, *Polym. Chem.* **2014**, *5*, 5211–5217.
[15] U. Rauwald, O. A. Scherman, *Angew. Chem. Int. Ed.* **2008**, *47*, 3950–3953; *Angew. Chem.* **2008**, *120*, 4014–4017.
[16] J. Liu, C. S. Y. Tan, Y. Lan, O. A. Scherman, *Macromol. Chem. Phys.* **2016**, *217*, 319–332.
[17] E. Pazos, P. Novo, C. Peinador, A. E. Kaifer, M. D. García, *Angew. Chem. Int. Ed.* **2019**, *58*, 403–416.
[18] H. Zou, J. Liu, Y. Li, X. Li, X. Wang, *Small* **2018**, *14*, 1–19.
[19] H. Qian, D. S. Guo, Y. Liu, *Chem. A Eur. J.* **2012**, *18*, 5087–5095.
[20] Y. Liu, H. Yang, Z. Wang, X. Zhang, *Chem. Asian J.* **2013**, *8*, 1626–1632.
[21] Z. Ji, J. Liu, G. Chen, M. Jiang, *Polym. Chem.* **2014**, *5*, 2709–2714.
[22] Z. Ji, J. Li, G. Chen, M. Jiang, *ACS Macro Lett.* **2016**, *5*, 588–592.
[23] E. A. Appel, F. Biedermann, U. Rauwald, S. T. Jones, J. M. Zayed, O. A. Scherman, *J. Am. Chem. Soc.* **2010**, *132*, 14251–14260.
[24] C. S. Y. Tan, J. Liu, A. S. Groombridge, S. J. Barrow, C. A. Dreiss, O. A. Scherman, *Adv. Funct. Mater.* **2018**, *28*, 1702994.
[25] J. Liu, C. S. Y. Tan, O. A. Scherman, *Angew. Chem. Int. Ed.* **2018**, *57*, 8854–8858.
[26] F. Tian, N. Cheng, N. Nouvel, J. Geng, O. A. Scherman, *Langmuir* **2010**, *26*, 5323–5328.
[27] P. E. Williams, Z. Walsh-Korb, S. T. Jones, Y. Lan, O. A. Scherman, *Langmuir* **2018**, *34*, 13104–13109.
[28] Y. J. Jeon, P. K. Bharadwaj, S. W. Choi, J. W. Lee, K. Kim, *Angew. Chem. Int. Ed.* **2002**, *41*, 4474–4476; *Angew. Chem.* **2002**, *114*, 4654–4656.
[29] L. Yang, H. Yang, F. Li, X. Zhang, *Langmuir* **2013**, *29*, 12375–12379.
[30] J. H. Mondal, S. Ahmed, D. Das, *Langmuir* **2014**, *30*, 8290–8299.
[31] J. H. Mondal, T. Ghosh, S. Ahmed, D. Das, *Langmuir* **2014**, *30*, 11528–11534.
[32] J. H. Mondal, S. Ahmed, T. Ghosh, D. Das, *Soft Matter* **2015**, *11*, 4912–4920.
[33] Y. H. Ko, I. Hwang, H. Kim, Y. Kim, K. Kim, *Chem. Asian J.* **2015**, *10*, 154–159.
[34] J. Kim, I. S. Jung, S. Y. Kim, E. Lee, J. K. Kang, S. Sakamoto, K. Yamaguchi, K. Kim, *J. Am. Chem. Soc.* **2000**, *122*, 540–541.
[35] M. C. Grenier, R. W. Davis, K. L. Wilson-Henjum, J. E. Ladow, J. W. Black, K. L. Caran, K. Seifert, K. P. C. Minbiole, *Bioorg. Med. Chem. Lett.* **2012**, *22*, 4055–4058.
[36] Y. H. Ko, H. Kim, Y. Kim, K. Kim, *Angew. Chem.* **2008**, *120*, 4174–4177; *Angew. Chem. Int. Ed.* **2008**, *47*, 4106–4109.
[37] K. Baek, Y. Kim, H. Kim, M. Yoon, I. Hwang, Y. H. Ko, K. Kim, *Chem. Commun.* **2010**, *46*, 4091–4093.
[38] R. Aav, K. A. Mishra, *Symmetry* **2018**, *10*, 98.
[39] X. Xiao, J. X. Liu, Z. F. Fan, K. Chen, Q. J. Zhu, S. F. Xue, Z. Tao, *Chem. Commun.* **2010**, *46*, 3741–3743.
[40] W. Kabsch, *Acta Crystallogr. D. Biol. Crystallogr.* **2010**, *66*, 125–132.
[41] W. Kabsch, *Acta Crystallogr. Sect. D* **2010**, *66*, 133–144.
[42] G. M. Sheldrick, *Acta Crystallogr. Sect. A* **2015**, *71*, 3–8.
[43] G. M. Sheldrick, *Acta Crystallogr. Sect. A* . **2008**, *64*, 112–122.
[44] L. J. Farrugia, *J. Appl. Crystallogr.* **2012**, *45*, 849–854.

Manuscript received: January 7, 2021
Revised manuscript received: February 3, 2021
Accepted manuscript online: February 10, 2021